

# Dalton Transactions

An international journal of inorganic chemistry

Accepted Manuscript

This article can be cited before page numbers have been issued, to do this please use: T. Ajaykamal, M. Sharma, N. S. Islam and M. Palaniandavar, *Dalton Trans.*, 2021, DOI: 10.1039/D1DT00299F.



This is an Accepted Manuscript, which has been through the Royal Society of Chemistry peer review process and has been accepted for publication.

Accepted Manuscripts are published online shortly after acceptance, before technical editing, formatting and proof reading. Using this free service, authors can make their results available to the community, in citable form, before we publish the edited article. We will replace this Accepted Manuscript with the edited and formatted Advance Article as soon as it is available.

You can find more information about Accepted Manuscripts in the [Information for Authors](#).

Please note that technical editing may introduce minor changes to the text and/or graphics, which may alter content. The journal's standard [Terms & Conditions](#) and the [Ethical guidelines](#) still apply. In no event shall the Royal Society of Chemistry be held responsible for any errors or omissions in this Accepted Manuscript or any consequences arising from the use of any information it contains.

## ARTICLE

## Rapid Atmospheric Carbon Dioxide Fixation by Nickel(II) Complexes: Meridionally Coordinated Diazepane-based 3N Ligands Facilitate Fixation

Tamilarasan Ajaykamal,<sup>a</sup> Mitu Sharma,<sup>b</sup> Nasreen S. Islam<sup>b</sup> and Mallayan Palaniandavar<sup>a\*</sup>

Received 00th January 20xx,  
Accepted 00th January 20xx

DOI: 10.1039/x0xx00000x

Octahedral complexes of the type  $[\text{Ni}(\text{L})(\text{H}_2\text{O})_3](\text{ClO}_4)_2$  **1**, **2**, where L is the tridentate 3N ligand 4-methyl-1-(pyrid-2-ylmethyl)-1,4-diazacycloheptane (**L1**, **1**), or 4-methyl-1-(*N*-methylimidazolyl)-1,4-diazacycloheptane (**L2**, **2**), have been isolated and characterized using elemental analysis, ESI-MS and electronic absorption spectroscopy. The DFT optimized structures of **1** and **2** reveal that the tridentate 3N ligands are coordinated meridionally constituting a distorted octahedral coordination geometry around nickel(II). In methanol solution, the complexes, upon treatment with triethylamine, generate the reactive red colored low-spin square planar Ni–OH intermediate  $[\text{Ni}(\text{L1/L2})(\text{OH})]^+$  (**1a**, **2a**), as characterized by ESI-MS and electronic absorption spectroscopy, and energy minimized structures. The latter when exposed to atmosphere rapidly absorbs atmospheric  $\text{CO}_2$  to produce the carbonate bridged dinickel(II) complexes  $[\text{Ni}_2(\text{L1/L2})_2(\mu\text{-CO}_3)(\text{H}_2\text{O})_2](\text{ClO}_4)_2$  (**3**, **4**), as characterized by elemental analysis and IR spectral feature ( $\sim 1608\text{ cm}^{-1}$ ) characteristic of bridging carbonate. Single crystal X-ray structure of **3** reveals the presence of a dinickel(II) core bridged by a carbonate anion in a symmetric mode. Both the Ni(II) centers are identical to each other with each Ni(II) possessing a distorted octahedral coordination geometry constituted by the meridionally coordinated 3N ligand, a carbonate ion and a water molecule. The kinetics decay of the red intermediates generated by **1** ( $k_{\text{obs}}, 7.7 \pm 0.1 \times 10^{-5}\text{ s}^{-1}$ ) and **2** ( $k_{\text{obs}}, 5.8 \pm 0.3 \times 10^{-4}\text{ s}^{-1}$ ) in basic methanol solution with atmospheric  $\text{CO}_2$  has been determined by absorption spectroscopy. DFT studies illustrate that meridional coordination of the 3N ligand and the electron-releasing imidazole ring as in **2** facilitate fixation of  $\text{CO}_2$ . The carbonate complex **3** efficiently catalyzes the conversion of styrene oxide into cyclic carbonate by absorbing atmospheric and pure  $\text{CO}_2$  with excellent selectivity.

### Introduction

The concentration of the greenhouse gas carbon dioxide in our atmosphere is ever-increasing due to continuous combustion processes and this contributes enormously to global warming and climate change. Currently, numerous investigations around the world are aimed at overcoming the serious environmental problems caused by  $\text{CO}_2$ . Investigations on the use of enzymatic,<sup>1a,2,3</sup> chemical,<sup>1b,c</sup> photochemical,<sup>1d</sup> and electrochemical<sup>4a</sup> methods have been undertaken to lower the concentration of  $\text{CO}_2$  in the atmosphere by capturing and fixing it. The development of effective chemical methods by activating and fixing atmospheric  $\text{CO}_2$  into useful organic compounds has gained a lot of significant attention currently.<sup>4-5</sup> Apart from fixing it, its conversion to carbonate is very important as many minerals exist as their carbonates<sup>1,6-7</sup> on the earth's crust. In nature, the zinc-containing enzyme

carbonic anhydrase<sup>2-3,8-9</sup> activates and converts  $\text{CO}_2$  to carbonic acid and the nickel-containing carbon monoxide dehydrogenase<sup>10-11</sup> (CODH) catalyzes the oxidation of CO to  $\text{CO}_2$ , followed by reduction of  $\text{CO}_2$  to CO. Also, dinuclear metalloenzymes like the nickel containing urease<sup>12</sup> are known to selectively bind  $\text{CO}_2$  and catalyze the hydrolysis of urea as well as redox reactions at ambient conditions.

In spite of its importance, only a limited number of chemical methods of fixing  $\text{CO}_2$  and converting it into valuable added products has been investigated. Coordination complexes of many metal ions like iron,<sup>13-14</sup> copper,<sup>15-16</sup> nickel<sup>25,26</sup> etc are known to activate atmospheric  $\text{CO}_2$  and fix it as useful organic compounds like cyclic carbonates. Among them, nickel complexes have attracted a lot of attention currently.<sup>17-26</sup> Very recently, certain dinickel azacryptand complexes<sup>17</sup> have been reported to selectively and reversibly bind  $\text{CO}_2$ . Also, complexes comprising Ni–OH moiety are known to facilitate  $\text{CO}_2$  fixation.<sup>18-24</sup> However, only a few Ni–OH systems exist that selectively bind  $\text{CO}_2$  between two nickel centers. Thus, the dinuclear Ni(II) complex<sup>20</sup>  $[(\text{TPA})\text{Ni}(\text{OH})_2\text{Ni}(\text{TPA})](\text{ClO}_4)_2$ , where TPA is tris(pyriylmethyl)amine, reacts with atmospheric  $\text{CO}_2$  to form the carbonate complex  $[(\text{TPA})\text{Ni}(\text{CO}_3)\text{Ni}(\text{TPA})](\text{ClO}_4)_2$ . Huang et al. found that Ni(II)-hydroxide complexes of 2,6-

<sup>a</sup> School of Chemistry, Bharathidasan University, Tiruchirappalli 620024, Tamil Nadu, India. E-mail: palanim51@yahoo.com

<sup>b</sup> Department of Chemical Sciences, Tezpur University, Tezpur, Assam, India

\*Electronic Supplementary Information (ESI) available: CCDC 1956983 (**3**). Characterization of complexes, crystallographic, computational and kinetics data are available as supplementary information. See DOI: 10.1039/x0xx00000x

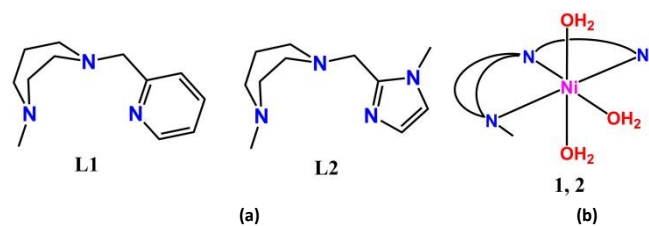


**Figure 1** a) Molecular structures of the tridentate 3N ligands L1 and L2 employed in this study and b) the octahedral coordination geometries of  $[\text{Ni}(\text{L1})(\text{H}_2\text{O})_3](\text{ClO}_4)_2$  **1** and  $[\text{Ni}(\text{L2})(\text{H}_2\text{O})_3](\text{ClO}_4)_2 \cdot 2\text{H}_2\text{O}$ .

pyridinedicarboxamidate dianion fix  $\text{CO}_2$  very efficiently.<sup>22,23</sup> The rapid fixation of atmospheric  $\text{CO}_2$  by hydroxo metal complexes is of special interest, because the fundamental understanding and application of the reaction may lead to some practical methods of not only reducing the atmospheric  $\text{CO}_2$  but converting it into useful compounds, in addition to illustrating the molecular mechanism of metalloenzyme activities and biomineralization. Also, the carbonate complexes have been shown<sup>25</sup> to catalyze the conversion of atmospheric  $\text{CO}_2$  into cyclic carbonate, and the reaction is important as it involves resource utilization, apart from having 100% atom economy. The cyclic carbonates find wide use as chemical intermediates,<sup>27</sup> sustainable aprotic solvents<sup>28</sup> and electrolytes in Li-ion batteries.<sup>29</sup>

Herein we describe our serendipitous discovery of spontaneous absorption and fixation of atmospheric  $\text{CO}_2$  by the in situ generated mononuclear Ni–OH complexes of the diazepane-based tridentate 3N pincer ligands L1 and L2 (Fig. 1) during our studies on bis( $\mu$ -hydroxido)nickel(II) complexes as catalysts for alkane hydroxylation. The products of the reaction are dinuclear Ni(II) complexes in which two nickel(II) atoms are bridged by a carbonate anion. Interestingly, the  $\text{CO}_2$  fixing capability of the Ni-hydroxo complex with a strongly electron-releasing *N*-Me-imidazole donor (L2) is higher than that of the complex with a pyridyl donor. DFT studies on the complexes and the red intermediates illustrate the difference in reactivity. The  $\mu$ -carbonato complex of L1 has been found to catalyze the conversion of styrene oxide into phenylethylene by absorption of atmospheric  $\text{CO}_2$ .

## Experimental

### Materials

Pyridine-2-carboxaldehyde, 1-methylimidazole-2-carboxaldehyde, *N*-methyl-homopiperazine, nickel(II) perchlorate hexahydrate (Aldrich), sodium triacetoxy borohydride, sodium hydride (Alfa Aesar), ethyl acetate, hexane, THF, triethylamine, phosphorus pentoxide, sodium hydroxide, sodium bicarbonate and sodium sulphate (Sisco Research Laboratory, India) were used as received. Dichloromethane, acetonitrile (Merck, India) and methanol (Sisco Research Laboratory, Mumbai) were distilled before use. The supporting electrolyte *tetra-N*-butylammonium perchlorate (Aldrich) was recrystallized and used.

### Synthesis of ligands

#### 4-Methyl-(1-pyrid-2-ylmethyl)-1,4-diazacycloheptane (L1)

This ligand was reported by one of us earlier.<sup>30</sup> In the present work, it was prepared by adopting the procedure used by one of us elsewhere for preparing 4-methyl-(1-pyrid-2-ylmethyl)-1,4-diazacycloheptane.<sup>31</sup> To a solution of *N*-methylhomopiperazine (1.14 g, 10 mmol) and pyridine-2-carboxaldehyde (1.07 g, 10 mmol) in  $\text{CH}_2\text{Cl}_2$  (100 mL) was added sodium triacetoxyborohydride with stirring (4.24 g, 20 mmol). The mixture obtained was stirred for 12 h, a saturated solution of  $\text{NaHCO}_3$  was added, and the stirring continued for a further 15 min. Then the solution was extracted with ethyl acetate, and the organic layer was dried over  $\text{Na}_2\text{SO}_4$ , filtered and rotaevaporated to dryness. The product was dissolved in THF (50 mL) and treated with NaH (0.72 g, 30 mmol) to remove traces of pyridyl-2-carbinol. After stirring the mixture for 90 min, the solvent was removed, and the residue extracted with several portions of hexane. The hexane extracts were combined, and the hexane removed to obtain L1 as brown oil which was used for preparing the complex **1**. Yield: 1.03 g (46%).  $^1\text{H}$  NMR (400 MHz,  $\text{CDCl}_3$ ):  $\delta$  7.49 (m, 1H), 7.22 (m, 1H), 6.97 (m, 2H), 4.65 (s, 2H), 3.70 (s, 4H), 2.68 (m, 4H), 2.46 (d, 3H), 1.75 (m, 2H). Anal. Calcd. for  $\text{C}_{12}\text{H}_{19}\text{N}_3$ : C, 70.20; H, 9.33; N, 20.47. Found: C, 70.15; H, 9.48; N, 20.37. HR-MS (MeOH) displays a peak at  $m/z$  206.1651 [ $\text{C}_{12}\text{H}_{20}\text{N}_3^+$ ] (cal. 206.1652) (Fig. S18).

#### 4-Methyl-1-(*N*-methylimidazol-2-ylmethyl)-1,4-diazacycloheptane (L2)

This ligand was synthesized by employing the procedure<sup>31</sup> used for preparing L1. To a solution of *N*-methylhomopiperazine (1.14 g, 10 mmol) and 1-methylimidazole-2-carboxaldehyde (1.10 g, 10 mmol) in  $\text{CH}_2\text{Cl}_2$  (100 mL) was added sodium triacetoxyborohydride (4.24 g, 20 mmol). The resulting mixture was stirred for 12 h, a saturated solution of  $\text{NaHCO}_3$  added, and the stirring continued for a further 15 min. The solution was then extracted with ethyl acetate, and the organic layer dried over  $\text{Na}_2\text{SO}_4$ , filtered and rotaevaporated to dryness. The oily product was dissolved in THF (50 mL) and treated with NaH (0.72 g, 30 mmol) to remove traces of imidazole carbinol. After stirring the mixture for 90 min, the solvent was rotaevaporated, and the residue extracted with several portions of hexane. The hexane extracts were combined, and the hexane removed to obtain L2 as brown oil which was used for preparing the complex **2**. Yield: 1.1 g (49%).  $^1\text{H}$  NMR (400 MHz,  $\text{CDCl}_3$ ):  $\delta$  6.93 (s, 1H), 6.87 (s, 1H), 4.90 (s, 5H), 4.13 (d, 4H), 2.68 (m, 5H), 2.38 (s, 2H), 1.85 (m, 2H). Anal. Calcd. for  $\text{C}_{11}\text{H}_{20}\text{N}_4$ : C, 63.43; H, 9.68; N, 26.90. Found: C, 63.50; H, 9.75; N, 26.77. HR-MS (MeOH) displays a peak at  $m/z$  209.1770 [ $\text{C}_{11}\text{H}_{20}\text{N}_4^+$ ] (cal. 209.1761) (Fig. S19).

#### Isolation of complex $[\text{Ni}(\text{L1})(\text{H}_2\text{O})_3](\text{ClO}_4)_2$ (**1**)

A methanol solution (5 mL) of  $\text{Ni}(\text{ClO}_4)_2 \cdot 6\text{H}_2\text{O}$  (0.365 g, 1 mmol) was added with stirring to a methanol solution (5 mL) of L1 (0.205 g, 1 mmol) at room temperature. The color of the solution turned green and the solution stirred for 8 hours. The precipitate obtained was filtered off, washed with small amounts of cold methanol and dried over  $\text{P}_2\text{O}_5$  under vacuum.

Yield, 0.41 g, 72%.  $\lambda_{\text{max}}/\text{nm}$ , in MeOH ( $\epsilon_{\text{max}}/\text{dm}^3 \text{ mol}^{-1}$ ): 941 (105), 618 (80), 361sh. Anal. Calcd. for  $\text{C}_{12}\text{H}_{25}\text{N}_3\text{Cl}_2\text{NiO}_{11}$ : C, 27.88; H, 4.87; N, 8.13. Found: C, 27.75; H, 4.60; N, 8.22. HR-MS (MeOH) displays a peak at  $m/z$  322.1074,  $[\text{M} + \text{Na} - \text{H}_2\text{O} - (\text{ClO}_4)_2]^{3+}$  (cal. 322.1041) (Fig. S20).

#### Isolation of complex $[\text{Ni}(\text{L2})(\text{H}_2\text{O})_3](\text{ClO}_4)_2 \cdot 2\text{H}_2\text{O}$ (2)

A methanolic solution (5 mL) of  $\text{Ni}(\text{ClO}_4)_2 \cdot 6\text{H}_2\text{O}$  (0.365 g, 1 mmol) was added with stirring to a methanol solution (5 mL) of L2 (0.208 g, 1 mmol) at room temperature. The solution turned green and was stirred for 8 hours. The precipitate obtained was filtered off, washed with small amounts of cold methanol and dried over  $\text{P}_2\text{O}_5$  under vacuum. Yield, 0.45 g, 84%.  $\lambda_{\text{max}}/\text{nm}$ , in MeOH ( $\epsilon_{\text{max}}/\text{dm}^3 \text{ mol}^{-1}$ ): 903 (35), 636 (30), 386sh. Anal. Calcd. for  $\text{C}_{11}\text{H}_{30}\text{N}_4\text{Cl}_2\text{NiO}_{13}$ : C, 23.76; H, 5.44; N, 10.08. Found: C, 23.50; H, 5.62; N, 10.15. HR-MS (MeOH) displays a peak at  $m/z$  356.7788,  $[\text{M} - (\text{ClO}_4)_2]^{2+}$  (cal. 356.1570) (Fig. S21).

#### Isolation of $[\text{Ni}_2(\text{L1})_2(\mu\text{-CO}_3)(\text{H}_2\text{O})_2](\text{ClO}_4)_2 \cdot 2\text{H}_2\text{O}$ (3)

**Method I:** A methanolic solution (5 mL) of  $\text{Ni}(\text{ClO}_4)_2 \cdot 6\text{H}_2\text{O}$  (0.365 g, 1 mmol) was added with stirring to a methanol solution (5 mL) of L1 (0.205 g, 1 mmol) at room temperature. The green solution was stirred for 30 min and then  $\text{Et}_3\text{N}$  (0.2 g, 2mmol) was added when the color of the solution turned red. The solution was stirred for two hours in open air atmosphere. The blue colored precipitate obtained was filtrated off, washed with small quantities of ice-cold methanol and then dried. Yield, 0.25 g, 44%.

**Method II:** A methanolic solution (5 mL) of  $\text{Et}_3\text{N}$  (0.2 g, 2 mmol) was added with stirring to a green methanolic solution (5 mL) of complex **1** (0.322 g, 1 mmol) at room temperature. The red solution obtained was stirred for two hours in open air atmosphere. The blue colored precipitate obtained was filtrated off, washed with small quantities of ice-cold methanol and then dried. Yield, 0.13 g, 58%.  $\lambda_{\text{max}}/\text{nm}$ , in MeOH ( $\epsilon_{\text{max}}/\text{dm}^3 \text{ mol}^{-1}$ ): 897 (180), 589 (125), 368sh. Anal. Calcd. for  $\text{C}_{25}\text{H}_{46}\text{N}_6\text{Cl}_2\text{Ni}_2\text{O}_{15}$ : C, 34.96; H, 5.40; N, 9.78. Found: C, 34.80; H, 5.42; N, 9.68. ATR ( $\nu$ ,  $\text{cm}^{-1}$ ): 1608 ( $\text{CO}_3^{2-}$ ). HR-MS (MeOH) displays a peak at  $m/z$  661.1806  $[\text{M} + \text{H}^+ - (\text{ClO}_4)_2]^{2+}$  (cal. 661.0728) (Fig. S25). Blue colored single crystals suitable for X-ray crystallographic analysis were obtained by slow evaporation of a  $\text{CH}_3\text{CN}/\text{CH}_3\text{OH}$  solution of the complex.

#### Isolation of $[\text{Ni}_2(\text{L2})_2(\mu\text{-CO}_3)(\text{H}_2\text{O})_2](\text{ClO}_4)_2$ (4)

**Method I:** A methanol solution (5 mL) of  $\text{Ni}(\text{ClO}_4)_2 \cdot 6\text{H}_2\text{O}$  (0.365 g, 1 mmol) was added with stirring to a methanol solution (5 mL) of L2 (0.208 g, 1 mmol) at room temperature. The solution turned green and was stirred for an additional 30 min with the addition of  $\text{Et}_3\text{N}$  (0.2 g, 2mmol). The color of the solution turned red and the solution further stirred for 30 min in open air atmosphere. The resulting green colored precipitate was filtrated off, washed with small quantities of ice-cold methanol and then dried.

**Method II:** A methanol solution (5 mL) of complex **2** (0.356 g, 1 mmol) was added with stirring to a methanol solution (5 mL) of  $\text{Et}_3\text{N}$  (0.2 g, 2mmol) at room temperature. The green solution was turned into red. The red color solution further stirred for 30 min in open air atmosphere. The resulting green colored precipitate was filtrated off, washed with small

quantities of ice-cold methanol and then dried. The complex **4** was insoluble in any solvent. Anal. Calcd. for  $\text{C}_{23}\text{H}_{44}\text{N}_8\text{Cl}_2\text{Ni}_2\text{O}_{13}$ : C, 33.33; H, 5.35; N, 13.52. Found: C, 33.40; H, 5.33; N, 13.42. ATR ( $\nu$ ,  $\text{cm}^{-1}$ ): 1615 ( $\text{CO}_3^{2-}$ ).

**Caution!** Perchlorate salts of the compounds are potentially explosive! Only small quantities of these compounds should be prepared and suitable precautions should be taken when they are handled.

#### General Procedure for Cyclic Carbonate Synthesis

A catalytic amount of the catalyst **3** (0.05 mol%) was dissolved in  $\text{CH}_3\text{CN}$  (2.0 mL) in a round bottom flask, and to this was added the epoxide styrene oxide (10 mmol) and  $\text{Et}_3\text{N}$  (6  $\mu\text{M}$ ) and the reaction vessel tightly closed with a rubber septum. Atmospheric air (1 bar pressure)/pure  $\text{CO}_2$  was passed through the reaction mixture heated to 30-80  $^\circ\text{C}$  for 8 h. The product formation was monitored by TLC for every 30 mins. After completion of the reaction the vessel was cooled to ambient temperature and the catalyst was removed by passing the reaction mixture through a silica-gel column. The product was identified as 4-phenyl-1,3-dioxolan-2-one by using  $^1\text{H}$  and  $^{13}\text{C}$  NMR and quantified by GC-MS/GC technique.

**4-Phenyl-1,3-dioxolan-2-one.**  $^1\text{H}$  NMR (400 MHz,  $\text{CDCl}_3$ ):  $\delta$ , 7.35-7.43 (m, 5H), 5.54-5.60 (t, 1H), 4.62-4.75 (m, 2H) ppm.  $^{13}\text{C}$  NMR (400 MHz,  $\text{CDCl}_3$ ):  $\delta$ , 154.70, 135.63, 129.06, 128.53, 125.63, 78.22, 71.03 ppm. GC-MS ( $m/z$ ): 164.10.

#### Physical measurements

$^1\text{H}$  NMR spectra were recorded on a Bruker 400 MHz NMR spectrometer. Chemical shifts for proton and carbon resonances are reported for the major isomer in parts per million (d) relative to tetramethylsilane (d 0.00) and chloroform (d 77.23) respectively. Multiplicities are indicated by singlet (s), doublet (d), triplet (t) and multiplet (m). UV-Visible and kinetic measurements were performed using a 1 cm cuvette on a Varian Cary 300 UV-Vis spectrophotometer. FT-IR spectra were obtained using solid samples with a Bruker ATR-Alpha (Diamond) spectrophotometer. Cyclic voltammetry (CV) and differential pulse voltammetry (DPV) on glassy carbon electrode were performed in MeOH at 25  $^\circ\text{C}$ . The voltammograms were generated using CH instruments 620C electrochemical analyzer. A three electrode system used to study the electrochemical behavior of complexes (0.001 M) consisted of a glassy carbon working electrode (A, 0.0707  $\text{cm}^2$ ), a platinum wire auxiliary electrode and a saturated calomel reference electrode and TBAP (0.1 M) was used as the supporting electrolyte. Solutions were deoxygenated by purging with nitrogen gas for 15 min prior to the measurement. Microanalyses (C, H and N) were carried out using PR 2400 Series II PerkinElmer equipment. High resolution mass analyses were performed using electron spray ionization (ESI) technique on a Thermo Scientific exactive plus EMR instrument. GC-MS and GC analysis were performed on Agilent 5977E GCMSD using HP-5 MS ultrainert (30 m  $\times$  250  $\mu\text{m}$   $\times$  0.25  $\mu\text{m}$ ) capillary column.

### Crystallographic data collection, refinement and structure solution

The molecular structures of the complex **3** was unambiguously determined by measuring the X-ray intensity data on a Bruker SMART APEX II single crystal X-ray CCD diffractometer having graphite-monochromatized Mo-K $\alpha$  ( $\lambda = 0.71073$  Å) radiation at ambient temperature. The structure was solved using direct methods with SHELXS-97 and refined using SHELXL-97, SHELXTL and SHELXL-2014, SHELXTL.<sup>41</sup> The graphics interface package used was PLATON, and the figures were generated using the ORTEP 3.07 generation package.<sup>42</sup> The positions on all the atoms were obtained by direct methods. Metal atoms in each complex were located from the E-maps and non-hydrogen atoms were refined anisotropically. The hydrogen atoms bound to the carbon were placed in geometrically constrained positions and refined with isotropic temperature factors, generally 1.2 Ueq of their parent atoms. Crystallographic data are listed in Table 1 and Table S1.

### Computational studies

DFT studies have been carried out to understand the effect of replacing pyridyl nitrogen by imidazolyl nitrogen on the capability of the tridentate ligands to involve in meridional coordination to Ni(II). The coordination geometries of Ni(II) complexes **1** and **2** with triplet spin in the ground state were fully optimized by using Density Functional Theory function (DFT) at U-B3LYP level of theory by employing Gaussian 09 program package.<sup>43</sup> The calculations were carried out with a mixed basis set of LanL2DZ for the nickel centre, which has a relativistic effective core potential with a valence basis set, and 6-31G for the remaining atoms.<sup>44-46</sup> The normal mode analyses were performed to check the minimal energy nature of the geometry. The complexes **1** and **2** were considered as dipositive cations while nickel metal was considered in +2 oxidation state. The solvation of the complexes was carried out by employing CPCM method using methanol as the solvent. The coordination geometries of Ni(II) intermediate complexes **1a** and **2a**, derived from **1** and **2** respectively, with singlet spin in the ground state were fully optimized by using Density Functional Theory function (DFT) at U-B3LYP level of theory by employing Gaussian 09 program package,<sup>39</sup> as described above for **1** and **2**. The complexes **1a** and **2a** were considered as monopositive cations while nickel metal was considered in +2 oxidation state. The solvation of the complexes was carried out by employing CPCM method using methanol as the solvent.

## Results and discussion

### Synthesis and characterization of ligands and complexes

The ligands 4-methyl-1-(pyrid-2-ylmethyl)-1,4-diazacycloheptane<sup>30</sup> (L1) and 4-methyl-1-(*N*-methylimidazolyl)-1,4-diaza-cycloheptane (L2) were prepared according to a known reductive amination procedure.<sup>31</sup> The nickel(II) complexes **1** and **2** were isolated in good yields as green solids by adding one equivalent of L1 or L2 to a methanol solution of one equivalent of Ni(ClO<sub>4</sub>)<sub>2</sub>·6H<sub>2</sub>O. They are formulated as

[Ni(L1)(H<sub>2</sub>O)<sub>3</sub>](ClO<sub>4</sub>)<sub>2</sub> **1** and [Ni(L2)(H<sub>2</sub>O)<sub>3</sub>](ClO<sub>4</sub>)<sub>2</sub>·2H<sub>2</sub>O **2** on the basis of elemental analysis, High Resolution Mass Spectrometry, conductivity measurements and UV-visible spectroscopy and the formulae supported by the energy minimized octahedral structures of cations of **1** and **2** (cf. below, Fig. 3). ESI-MS reveal that both **1** ( $m/z$  322.1074, [M + Na - H<sub>2</sub>O - (ClO<sub>4</sub>)<sub>2</sub>]<sup>3+</sup>) and **2** ( $m/z$  356.7788, [M - (ClO<sub>4</sub>)<sub>2</sub>]<sup>2+</sup>) remain as mononuclear complex species in solution. Such complexes are interesting but no single crystals of them could be grown to determine their molecular structures using X-ray diffraction. The dinickel(II) complexes **3** and **4** were prepared by adding one equivalent of the ligand L1 or L2 to a methanol solution of Ni(ClO<sub>4</sub>)<sub>2</sub>·6H<sub>2</sub>O to generate the complexes **1** and **2** in situ, followed by adding excess of Et<sub>3</sub>N in methanol, and exposing the red solution obtained to atmospheric CO<sub>2</sub>. They were also prepared by treating a methanolic solution of their parent complexes **1** and **2** by with Et<sub>3</sub>N and then exposing it to atmospheric CO<sub>2</sub>. They are formulated as [Ni<sub>2</sub>(L1/L2)<sub>2</sub>(μ-CO<sub>3</sub>)(H<sub>2</sub>O)<sub>2</sub>](ClO<sub>4</sub>)<sub>2</sub>·*n*H<sub>2</sub>O (**3**: *n*=2; **4**: *n*=0) on the basis of elemental analysis, High Resolution Mass Spectrometry ( $m/z$  661.1806 [M + H<sup>+</sup> - (ClO<sub>4</sub>)<sub>2</sub>]<sup>2+</sup>), and UV-visible spectroscopy, and the formula confirmed by the X-ray crystal structure of **3** (cf. below, Fig. 2). They can be synthesized also by bubbling CO<sub>2</sub> or by adding a carbonate salt to the red solution. The molar conductivity of **1**, **2** and **3** in methanol solution ( $\Lambda_m/\Omega^{-1}$  cm<sup>2</sup> mol<sup>-1</sup>: 237–260) fall in the range observed for 1:2 electrolytes.

### Description of the structure of [Ni<sub>2</sub>(L1)<sub>2</sub>(μ-CO<sub>3</sub>)(H<sub>2</sub>O)<sub>2</sub>](ClO<sub>4</sub>)<sub>2</sub>·4H<sub>2</sub>O **3**

The molecular structure of the complex cation of [Ni<sub>2</sub>(L1)<sub>2</sub>(μ-CO<sub>3</sub>)(H<sub>2</sub>O)<sub>2</sub>](ClO<sub>4</sub>)<sub>2</sub>·4H<sub>2</sub>O **3** is shown in Fig. 2 and the packing diagram shown in Fig. S2. It consists of a dinickel(II) core formed by bridging of two Ni(II) centers through a carbonate anion. Both the Ni(II) centers are identical to each other with each Ni(II) possessing a distorted octahedral coordination geometry constituted by the three nitrogen atoms of meridionally coordinated L1, two oxygen atoms of the bridging CO<sub>3</sub><sup>2-</sup>, and the oxygen atom of a water molecule. The meridional coordination of L1 is similar to that observed in the copper(II) complex [Cu(L1)Cl<sub>2</sub>].<sup>32</sup> The diazepane backbone of the tridentate 3N ligand accounts for its meridional coordination to Ni(II), which is in contrast to the facial coordination of the tridentate ligand bis(pyrid-2-ylmethyl)(*tert*-butyl)amine (*t*Bu-DPA) to Ni(II).<sup>21</sup> This is interesting as 3N ligands with two pyridyl donors like bis(pyrid-2-ylmethyl)amine (DPA)<sup>33-35</sup> and *t*BuDPA<sup>21</sup> are involved in the more commonly adopted *cis*-facial<sup>34,35</sup> rather than meridional coordination. The Ni–N<sub>amine</sub> (2.082(4), 2.107(4) Å) and Ni–N<sub>py</sub> (2.068(4) Å) bond lengths (Table 1) fall in the ranges observed already for similar Ni(II) complexes.<sup>20,37</sup> The carbonate ion is bound to both the Ni(II) centers in a μ<sub>2</sub>-κ<sup>2</sup>:κ<sup>2</sup> mode,<sup>20,26</sup> with the Ni–O(CO<sub>3</sub><sup>2-</sup>) bond lengths being 2.088(3) and 2.073(4) Å. The C–O bond lengths (C–O2, 1.281(4), C–O2a, 1.281(4), C–O3, 1.304(6) Å) suggest that the bound carbonate ion is strongly delocalized. Also, the two pyridyl moieties are oriented in

directions opposite to each other and the two coordinated water molecules are also

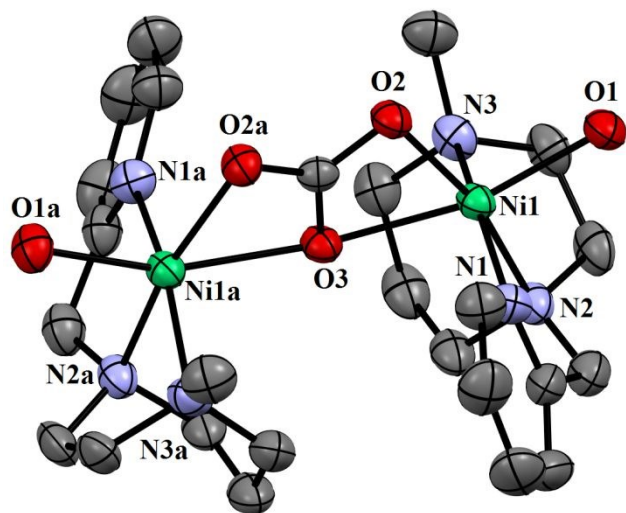


**Figure 2** ORTEP diagram of complex cation of **3** showing 50% probability thermal ellipsoids and the labeling scheme for selected atoms. All the hydrogen atoms, solvent molecules and the perchlorate counter ions are omitted for clarity.

**Table 1** Selected bond lengths [Å] and bond angles [°] for  $[\text{Ni}_2(\text{L1})_2(\mu\text{-CO}_3)(\text{H}_2\text{O})_2](\text{ClO}_4)_2 \cdot 4\text{H}_2\text{O}$  **3**

Bond lengths [Å]		Bond Angle [°]	
Ni1–N1	2.068(4)	O1–Ni1–O2	60.98(11)
Ni1–N2	2.082(4)	O1–Ni1–O3	159.04(13)
Ni1–N3	2.107(4)	O2–Ni1–O3	98.24(12)
Ni1–O1	2.2641(11)	N1–Ni1–N2	82.83(15)
Ni1–O2	2.088(3)	N2–Ni1–N3	77.53(15)
Ni1–O3	2.073(4)	N1–Ni1–N3	160.09(15)
		N3–Ni1–O3	91.82(16)
		N1–Ni1–O1	86.53(11)

oriented similarly, which has implications for the proposed mechanism of  $\text{CO}_2$  fixation (cf. below). Such a compact coordination geometry of **3** with the diazepane backbone accounts for the spontaneous and rapid fixation of atmospheric  $\text{CO}_2$  by **1** and **2**. A comparison of the structure of **3** with that of **4** would have thrown light on their formation

and reactivities but unfortunately, we failed in our attempts to obtain single crystals of **4**.

#### DFT studies: Structures of nickel(II) complexes **1**, **2** and intermediates **1a**, **2a**

The optimized geometries of cations of the complexes **1** and **2** have been computed using density functional theory (DFT). The optimized structures of the complexes are shown in Figs 3 and 4, and the geometrical parameters viz. bond lengths, optimized energies, frontier MOs, and HOMO–LUMO energy gaps have been calculated (Table 2, S2, S3 and S4; Fig. 5, 6, 7 and S15, 16<sup>†</sup>) at B3LYP hybrid exchange–correlation function with 6-31G/LANL2DZ combined basis sets using Gaussian 09 program package. The distorted octahedral coordination geometries of Ni(II) cations are constituted by all the three nitrogen atoms of meridionally coordinated L1 and L2, and the oxygen atoms of three water molecules. The Ni–N<sub>amine</sub> (**1**: 2.140, 2.115; **2**: 2.132, 2.149 Å), Ni–N<sub>py</sub> (2.077 Å) and Ni–N<sub>im</sub> (2.059 Å) bond lengths (Table 2) fall in the ranges observed already for similar Ni(II) complexes,<sup>37,38</sup> suggesting that the optimized structures are reliable and can be used to understand the structural variations and reactivity. Of the three Ni–O bonds, the one (Ni–O1, 2.088 Å) trans to Ni–N2 is much shorter than the other two (Ni–O2, 2.152; Ni–O3, 2.136 Å). To understand the difference in reactivities of **1** and **2** towards  $\text{CO}_2$ , the optimized geometries of the red intermediates  $[\text{Ni}(\text{L1})(\text{OH})]^+$  **1a** and  $[\text{Ni}(\text{L2})(\text{OH})]^+$  **2a**, obtained (cf. below) by treating respectively **1** and **2** in methanol solution with triethylamine, have been also computed (Fig. 4).

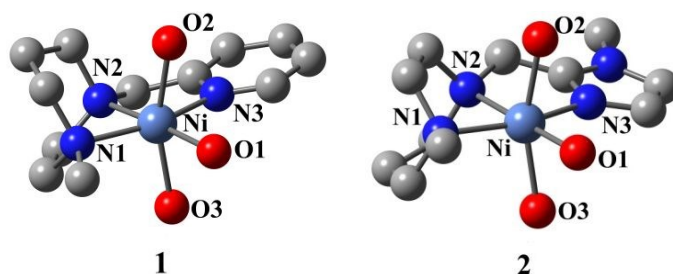


**Figure 3** The computed coordination structures of cations of  $[\text{Ni}(\text{L1})(\text{H}_2\text{O})_3](\text{ClO}_4)_2$  **1** and  $[\text{Ni}(\text{L2})(\text{H}_2\text{O})_3](\text{ClO}_4)_2 \cdot 2\text{H}_2\text{O}$  **2**.

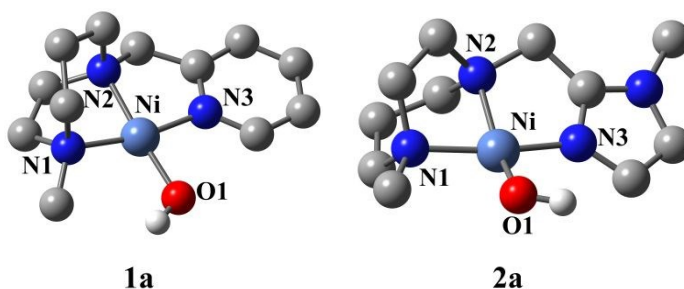


**Figure 4** The energy minimized structures computed for the cationic intermediate species  $[\text{Ni}(\text{L1})(\text{OH})]^+$  **1a** and  $[\text{Ni}(\text{L2})(\text{OH})]^+$  **2a**.

**Table 2** Computed structural parameters and values of the HOMO–LUMO energy gap in complexes **1**, **2** and the intermediates **1a** and **2a**.

Parameters	<b>1</b>	<b>2</b>	<b>1a</b>	<b>2a</b>
<b>Bond lengths [Å]</b>				
Ni–N(1)	2.140	2.132	1.967	1.984
Ni–N(2)	2.115	2.149	1.960	1.996
Ni–N(3)	2.077	2.059	1.915	1.890
Ni–O(1)	2.088	2.086	1.844	1.842
Ni–O(2)	2.152	2.149	-	-
Ni–O(3)	2.136	2.132	-	-
Optimized energy (eV)	$-2.81 \times 10^4$	$-2.85 \times 10^4$	$-2.39 \times 10^4$	$-2.44 \times 10^4$
HOMO (eV)	-6.8415	-6.8254	-6.3604	-6.2700
LUMO (eV)	-1.9448	-0.5883	-1.8444	-1.6393
HOMO–LUMO energy gap (eV)	4.8967	6.2371	4.5160	4.6307

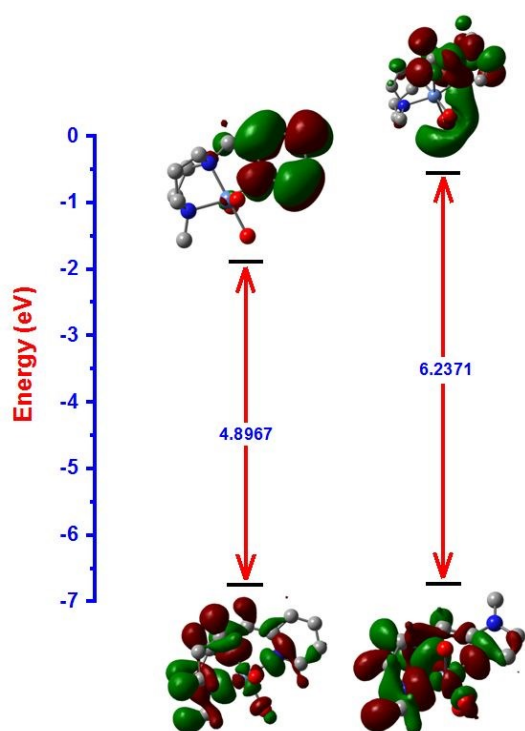


**Figure 5** HOMO and LUMO band gap Energy profile diagram for **1** and **2** were calculated in U-B3LYP level of theory with mixed basis sets LANL2DZ/6-31G and methanol as a solvent in CPCM method.

The intermediates possess low-spin square planar coordination geometry formed by the three nitrogen atoms of meridionally coordinated L1 and L2, and an oxygen atom of hydroxyl group. The Ni–N<sub>amine</sub> (**1**: 1.967, 1.960; **2**: 1.984, 1.996 Å), Ni–N<sub>py</sub> (1.915 Å) and Ni–N<sub>im</sub> (1.890 Å) bond lengths (Table 2) fall in the ranges observed for related square planar low-spin Ni(II) complexes in their X-ray crystal structures,<sup>25,38</sup> suggesting that the optimized structures of **1a** and **2a** are reliable and can be used to understand the reactivity and structural variations (Fig. 4, see in ESI<sup>†</sup>). Thus, upon formation of **1a** and **2a** from respectively **1** and **2**, all the Ni–N and Ni–O1 bond lengths in them decrease, illustrating that the nitrogen donor atoms come closer to Ni(II), facilitated by the diazepane back bone, to effect a higher ligand field strength and pair the electron spins in Ni(II) to give the low-spin ( $d_{xz}, d_{yz}$ )<sup>4</sup>( $d_{xy}$ )<sup>2</sup>( $d_{z^2}$ )<sup>2</sup> configuration. It is expected that the [Ni(L1/L2)(OH)]<sup>+</sup> species with the latter configuration would act as an electron-rich **super nucleophile**, like the reactive [(4N)Co]<sup>I</sup> species with ( $d_{xz}, d_{yz}$ )<sup>4</sup>( $d_{xy}$ )<sup>2</sup>( $d_{z^2}$ )<sup>2</sup> configuration, obtained by two-electron reduction of alkylcobalamin, towards electrophilic carbon atom of CO<sub>2</sub> (cf. below). The Ni–O1(H<sub>2</sub>O) bond length also decreases upon deprotonation from 2.088 (**1**) to 1.844 (**1a**) and 2.086 (**2**) to 1.842 (**2a**) Å, illustrating the stronger coordination of oxygen atom of hydroxyl group. Computations reveal that the electron-releasing imidazole donor in the former destabilizes<sup>39</sup> the HOMO orbital in **2a** (**1a**: -6.3604; **2a**: -6.2700 eV) relative to the pyridyl donor in **1a** (cf. above). Similarly, the LUMO in **2a** is more destabilized than that in **1a** (**1a**: -1.8444; **2a**: -1.6393 eV) with the HOMO – LUMO energy gap being lower in **1a** than in **2a** (**1a**: 4.5160; **2a**: 4.6307 eV). However, the HOMO – LUMO+1 energy gap in **1a** is higher

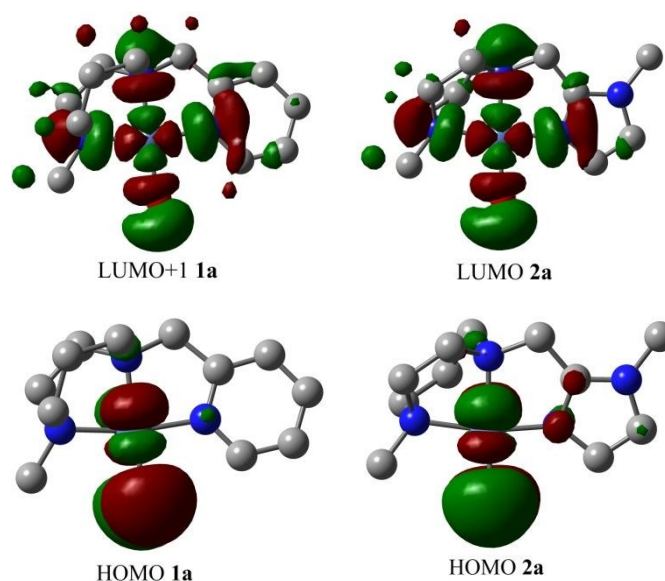


**Figure 6** Electron density plot of HOMO of intermediates **1a** and **2a**, LUMO+1 of **1a** and LUMO of **2a**.

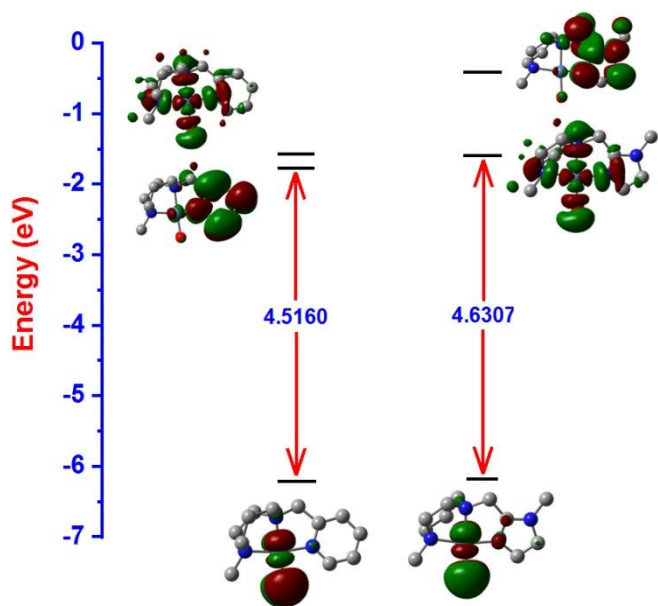


**Figure 7** HOMO and LUMO band gap Energy profile diagram for **1a** and **2a** were calculated in U-B3LYP level of theory with mixed basis sets LANL2DZ/6-31G and methanol as a solvent in CPCM method.

than the HOMO – LUMO energy gap in **2a** (**1a**: 4.7103; **2a**: 4.6307 eV), which is consistent with the higher energy of the CT band observed (cf. above) for **1a** (**1a**: 524; **2a**: 540 nm). It may be noted that they have similar electron density distribution. It may be noted that LUMO+1 in **1a** and LUMO in **2a** have similar electron density distribution (Fig. 6, 7).

#### Electronic absorption spectral and electrochemical properties

The electronic spectral features observed for **1** and **2** in methanol solution ( $\lambda_{\max}/\text{nm}$ ,  $\epsilon_{\max}/\text{dm}^3 \text{ mol}^{-1}$ : **1**, 941 (105), 618 (80), 361sh, **2**, 903 (35), 636 (29), 386sh, Table 3, Figure S4) reveal that the octahedral coordination geometries of the complexes are maintained in solution. The lowest energy band is assigned to  ${}^3A_{2g} \rightarrow {}^3T_{2g}(F)$  ( $v_1$ ) transition while the higher energy band to  ${}^3A_{2g} \rightarrow {}^3T_{1g}(F)$  ( $v_2$ ) transition in Ni(II) located in the octahedral environment. The intense shoulder observed around 360 (**1**) and 390 nm (**2**) is assigned to  ${}^3A_{2g} \rightarrow {}^3T_{1g}(P)$  ( $v_3$ ) transition. The lower intensity absorption spectral feature around 750 nm is assigned to  ${}^3A_{2g} \rightarrow {}^1E_{1g}(D)$  spin-forbidden transition. All these assignments are in good agreement with those observed for similar octahedral Ni(II) complexes reported previously.<sup>40</sup> The  $v_1$  band energy of **1** (941 nm) is lower than that of **2** (903 nm), which is expected of the more basic *N*-Me-imidazole nitrogen donor ( $pK_a$ :  $\text{pyH}^+$ , 5.2,  $\text{MeImH}^+$ , 7.0), and hence its stronger coordination in **2**. Also, the  $v_1$  band energy of **1** is higher than that (1096 nm) of  $[\text{Ni}(\text{tBuDPA})(\text{H}_2\text{O})_3](\text{ClO}_4)_2$ ,<sup>21</sup> which reveals that the diazepane backbone of the meridionally coordinated L1 confers a ligand field strength higher than the cis-facially coordinating *t*BuDPA. In methanol solution, the carbonate complex **3** displays well defined electronic absorption spectral features ( $\lambda_{\max}/\text{nm}$ ,

$\epsilon_{\max}/\text{dm}^3 \text{ mol}^{-1}$ : 897 (180), 589 (125), 368sh, Fig. 8 and Table 3) typical of octahedral coordination geometry around Ni(II). In  $\text{CH}_3\text{CN}$  solution, the  $v_1$  and  $v_2$  bands are slightly shifted ( $\lambda_{\max}/\text{nm}$ ,  $\epsilon_{\max}/\text{dm}^3 \text{ mol}^{-1}$ : 905 (165), 580 (95), 396sh, Table 3), revealing the stronger binding of  $\text{CH}_3\text{CN}$  solvent molecules to Ni(II). While the lowest energy band is assigned to  $v_1$  transition, the higher energy band to  $v_2$  transition and the intense highest energy band around 368 nm to  $v_3$  transition in Ni(II) located in an octahedral environment. The  $v_1$  band energy (897 nm) of **3** is higher than that of **1**, suggesting that the carbonate anion chelates more strongly in **3** contributing to the higher ligand field strength.

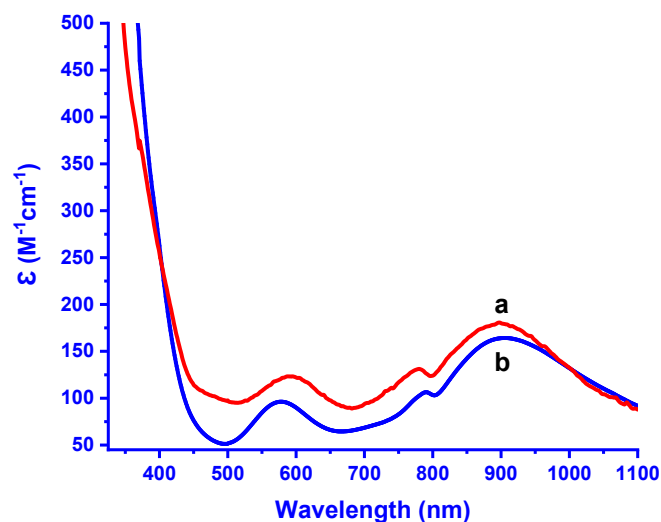


**Figure 8** Electronic absorption spectra of  $[\text{Ni}_2(\text{L}1)_2(\text{CO}_3)(\text{H}_2\text{O})_2](\text{ClO}_4)_2 \cdot 2\text{H}_2\text{O}$  **3** in (a) Methanol and (b) Acetonitrile solution at 25 °C.

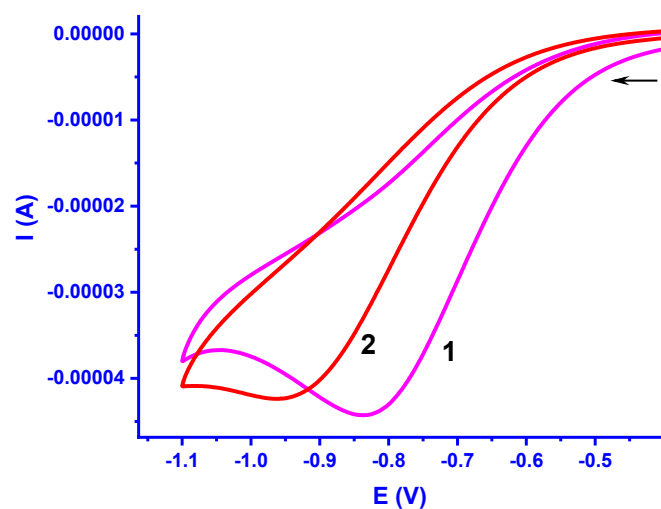


**Figure 9** Cyclic voltammograms of complexes **1** ( $1.9 \times 10^{-3} \text{ M}$ ) and **3** ( $1.8 \times 10^{-3} \text{ M}$ ) in methanol solution at 25 °C. Conditions: supporting electrolyte, 0.1 M TBAP; Scan rate, 50  $\text{mV s}^{-1}$ ; reference electrode, Calomel; working electrode, Glassy carbon; Counter electrode, platinum plate.

**Table 3** UV-visible spectral data of nickel(II) complexes **1**, **2**, **3** and intermediates **1a** and **2a** in CH<sub>3</sub>OH solvent at 25 °C.View Article Online  
DOI: 10.1039/D1DT00299F

Complex	Solvent	Electronic spectra		CV		DPV $E_{1/2}$ (V)
		Wavelength (nm)	$\epsilon$ (M <sup>-1</sup> cm <sup>-1</sup> )	$E_{pc}$ (V)	$E_{pc1/2}$ (V)	
[Ni(L1)(H <sub>2</sub> O) <sub>2</sub> ](ClO <sub>4</sub> ) <sub>2</sub> ( <b>1</b> )	Methanol	941 (v <sub>1</sub> )	105	-0.841	-0.663	-0.745
		618 (v <sub>2</sub> )	85			
		361 (v <sub>3</sub> )	sh			
[Ni(L2)(H <sub>2</sub> O) <sub>2</sub> ](ClO <sub>4</sub> ) <sub>2</sub> ·2H <sub>2</sub> O ( <b>2</b> )	Methanol	903 (v <sub>1</sub> )	35	-0.984	-0.781	-0.901
		636 (v <sub>2</sub> )	30			
		386 (v <sub>3</sub> )	sh			
[Ni <sub>2</sub> (L1) <sub>2</sub> (CO <sub>3</sub> )(H <sub>2</sub> O) <sub>2</sub> ](ClO <sub>4</sub> ) <sub>2</sub> ·2H <sub>2</sub> O ( <b>3</b> )	Methanol	897 (v <sub>1</sub> )	180	-0.960	-0.760	-0.825
		589 (v <sub>2</sub> )	125			
		376 (v <sub>3</sub> )	sh			
[Ni <sub>2</sub> (L1) <sub>2</sub> (CO <sub>3</sub> )(H <sub>2</sub> O) <sub>2</sub> ](ClO <sub>4</sub> ) <sub>2</sub> ·2H <sub>2</sub> O ( <b>3</b> )	Acetonitrile	905 (v <sub>1</sub> )	165	-	-	-
		577 (v <sub>2</sub> )	100			
		396 (v <sub>3</sub> )	sh			
[Ni(L1)(OH)] <sup>+</sup> <b>1a</b> intermediate	Methanol	474	3,700	-	-	-
		524	3,620			
[Ni(L2)(OH)] <sup>+</sup> <b>2a</b> intermediate	Methanol	463	1,310	-	-	-
		540	sh			

Conc. **1**:  $4.5 \times 10^{-3}$ , **2**:  $3.1 \times 10^{-3}$  M; **1a**, **2a**:  $2 \times 10^{-4}$ , **3**:  $7.6 \times 10^{-4}$  M in methanol; **3**,  $2.7 \times 10^{-3}$  M in acetonitrile solvent. Cyclic voltammograms and DPV of complexes **1** ( $1.9 \times 10^{-3}$  M), **2** ( $5.2 \times 10^{-3}$ ) and **3** ( $1.8 \times 10^{-3}$  M) in methanol. Conditions: supporting electrolyte, 0.1 M TBAP; Scan rate, CV: 50 mVs<sup>-1</sup>, DPV: 2 mVs<sup>-1</sup>, for all complexes, reference electrode, calomel; working electrode, glassy carbon.

The cyclic voltammetry (CV) responses obtained for **1** and **2** in methanol solution reveal that the Ni(II)/Ni(I) redox couples are completely irreversible, as no reoxidation wave is observed (Fig. 9, S5). The Ni(II)/Ni(I) redox potential of **2** is more negative than that of **1** ( $E_{1/2}$ : **1**, -0.745; **2**, -0.901 V vs calomel, DPV, Table 3), which is expected of the more basic *N*-Me-imidazole nitrogen donor (cf. above) and hence its stronger coordination in **2**. This is in agreement with the observation of v<sub>1</sub> band for **2** at energy higher than that for **1**. The Ni(II)/Ni(I) redox of **3** is irreversible ( $E_{1/2}$ : -0.825 V, Table 3), which is more negative than that of its monomeric Ni(II) complex **1**, which is consistent with the observation of the v<sub>1</sub> band at energy higher for **3** than that for **1**.

#### Carbon Dioxide Fixation: Characterization and reactivity of intermediate [Ni(L1/L2)(OH)]<sup>+</sup> species

When a methanolic solution of Ni(ClO<sub>4</sub>)<sub>2</sub>·6H<sub>2</sub>O was added with stirring to a solution of an equivalent amount of L1 in methanol at room temperature a green solution was obtained. The latter was treated with two equivalents of Et<sub>3</sub>N to give a red colored solution (pH, 10). Interestingly, when the latter

was stirred for two hours in an open atmosphere, a blue colored precipitate was obtained. The product was identified and formulated as [Ni<sub>2</sub>(L1)<sub>2</sub>(μ-CO<sub>3</sub>)(H<sub>2</sub>O)<sub>2</sub>](ClO<sub>4</sub>)<sub>2</sub>·2H<sub>2</sub>O **3**, which is confirmed by its X-ray crystal structure (Fig. 2). The sharp IR spectral feature observed around 1608 cm<sup>-1</sup> is characteristic of carbonate anion involved in symmetric μ-mode of coordination as found in the X-ray crystal structure.<sup>25,36</sup> When pure CO<sub>2</sub> gas was bubbled through the red solution, the color changed from red to green much faster than when exposed to atmospheric CO<sub>2</sub>, and the blue colored product obtained was identified as **3** by using its UV-Vis spectral features. When a methanolic solution of NaOH was used in the place of Et<sub>3</sub>N, a similar red coloured solution was formed and finally a blue precipitate of **3** was obtained. When a methanolic solution of the complex was acidified with dil. HCl, solvated Ni<sup>2+</sup> ions are formed, indicating that the complex **3** is unstable. However, when sodium hydroxide was added to a methanolic solution of **3** no change in the absorption spectrum was observed, revealing that the carbonate complex is stable in basic solution. The Ni(II) complex **4** of L2 isolated by adopting the procedure used for **3** was found to have the composition

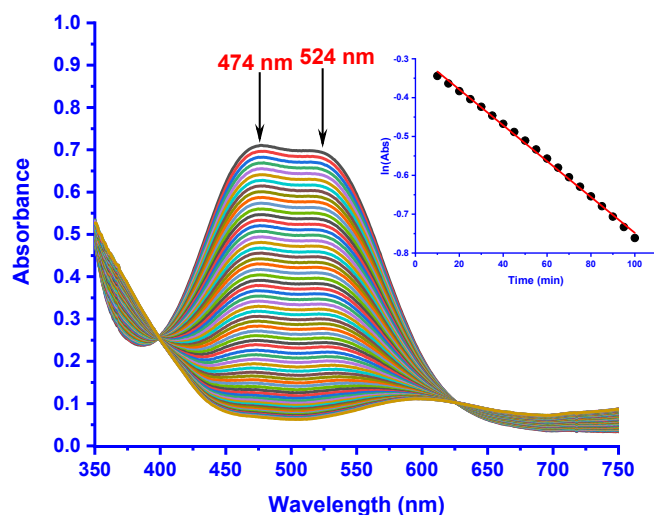
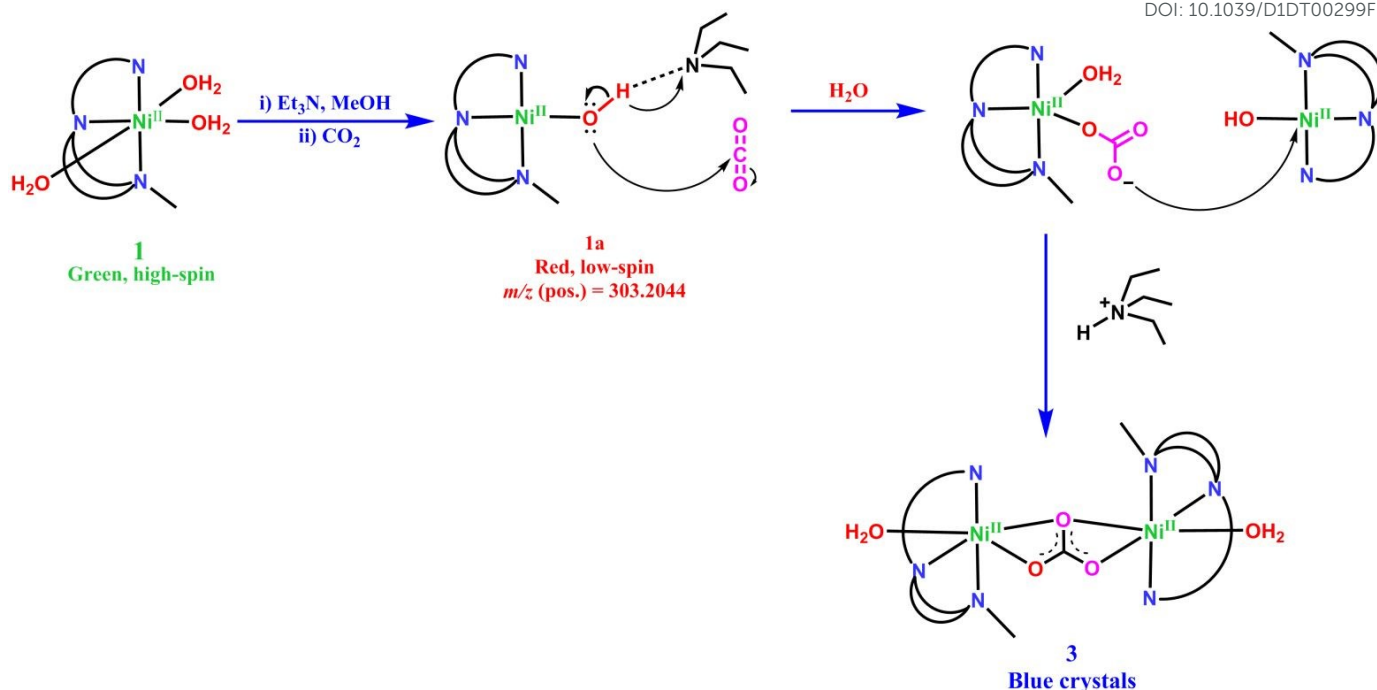


**Figure 10** Reaction of the intermediate  $[\text{Ni}(\text{L}1)(\text{OH})]^+$  **1a** upon exposure to atmospheric  $\text{CO}_2$  followed at 5 min interval. There are two isosbestic points at 400 and 625 nm. The intermediate was generated by adding  $\text{Et}_3\text{N}$  ( $4 \times 10^{-4}$  M) to complex **1** ( $2 \times 10^{-4}$  M). Inset: Plot of absorbance vs time, observed at 474 nm.  $k_{\text{obs}} = 7.7 \pm 0.1 \times 10^{-5} \text{ s}^{-1}$  ( $t_{1/2} = 2.5$  hrs).

$[\text{Ni}_2(\text{L}2)_2(\mu\text{-CO}_3)(\text{H}_2\text{O})_2](\text{ClO}_4)_2$ , same as that of **3** (Table 3). As it is insoluble in any solvent it was not studied further. It is possible that the coordination of the more basic and smaller imidazole donor in L2 causes efficient packing in the solid state resulting in insolubility of **4**. When the red colored solution obtained upon adding two equivalents of  $\text{Et}_3\text{N}$  to one equivalent of  $[\text{Ni}(\text{L}1)(\text{H}_2\text{O})_3]^{2+}$  **1** was subjected to ESI-MS analysis a mass peak at  $m/z$  (pos.) = 303.2044 was observed (Fig. S22), which agrees well with the value of  $m/z$  = 303.0858 calculated for the intermediate Ni(II)-hydroxyl species  $[\text{Ni}(\text{L}1)(\text{OH})+\text{Na}]^{2+}$ . The same intermediate species was generated in basic ethanol ( $m/z$ , 303.2050, Fig. S23) and isopropanol ( $m/z$ , 303.2046, Fig. S24) solutions but not in basic acetonitrile and DMF solutions. When a small amount of methanol was added to the green solution of **1** in basic ( $\text{Et}_3\text{N}$ ) acetonitrile or DMF solution, the solution became red in color characteristic of the  $[(\text{L}1/\text{L}2)\text{Ni}(\text{II})\text{-OH}]$  species **1a** and **2a**. All these observations reveal that alcoholic solvents stabilize the Ni(II)-hydroxo intermediate by hydrogen-bonding possibly with the hydroxyl group coordinated to the intermediate species  $[\text{Ni}(\text{L}1)(\text{OH})]^+$ . The magnetic moments of **1** and **1a** in methanol solution were determined by using Evans' method (Fig. S3).<sup>49</sup> While **1** is found to be paramagnetic ( $\mu_{\text{eff}}$ , 2.93 BM) **1a** is diamagnetic. The latter possesses a low-spin square planar configuration, as diagnosed from the red color, magnetic moment determined by Evan's method and the presence of intense absorption bands around 474 and 524 nm observed selectively in alcoholic solvents and absence of bands characteristic of octahedral ligand field. The former band is assignable to  ${}^1\text{A}_{1g} \rightarrow {}^1\text{A}_{2g}$  ligand field transition in Ni(II) with a square planar coordination geometry, and the other one

possibly to a metal to ligand charge transfer (MLCT) transition. We have already established the ability of the related diazepane-based 4N ligands *N,N'*-bis(2-pyrid-2-ylmethyl)-1,4-diazacycloheptane and *N,N'*-bis((1-methyl-1H-imidazole-2-yl)methyl)-1,4-diaza-cycloheptane to impose a low-spin configuration on Ni(II).<sup>25,38</sup> A similar mononuclear square planar complex  $[(\text{L}3)\text{Ni}^{\text{II}}\text{-OH}]^-$ , where L3 is the diacidic tridentate 3N ligand 2,6-pyridinedicarboximate, has been prepared, characterized ( $\lambda_{\text{max}}$ , 411, 490 nm) and X-ray structure determined.<sup>23,24</sup> When  $\text{N}_2$  gas was purged continuously for an hour through solutions of **1** and **2** in methanol to remove any dissolved dioxygen, and then  $\text{Et}_3\text{N}$  was added, the red solutions characteristic of the intermediate species **1a** and **2a** were generated. When dioxygen was bubbled through this red solution no change was observed, suggesting that the intermediate is stable towards dioxygen. We were able to obtain the electronic absorption spectrum (436, 540sh nm) of the red colored  $[\text{Ni}(\text{L}2)(\text{OH})]^+$  species **2a** generated in situ from **2**, but not its HR-MS as it is very reactive (cf. below).

The kinetics of decay of the  $[\text{Ni}(\text{L}1/\text{L}2)(\text{OH})]^+$  intermediates, generated in situ upon adding  $\text{Et}_3\text{N}$  in methanol to a methanolic solution of **1** and **2**, upon exposure to atmospheric air to give **3** and **4** was followed by monitoring the decreases in intensity of the intense bands around 474 nm for **1** (Fig. 10) and that around 463 nm for **2** (Fig. S12, S13). The plots of absorbance vs time for both **1** ( $k_{\text{obs}}$ ,  $7.7 \pm 0.1 \times 10^{-5} \text{ s}^{-1}$ ;  $t_{1/2}$ , 2.5 hrs) and **2** ( $k_{\text{obs}}$ ,  $5.8 \pm 0.3 \times 10^{-4} \text{ s}^{-1}$ ;  $t_{1/2}$ , 0.33 hrs) are linear, showing that the intermediate **2a** reacts with excess  $\text{CO}_2$  almost 10 times faster than **1a** in methanol. It may be noted that **4** was formed instantaneously in basic solution upon exposure of **2** to atmospheric  $\text{CO}_2$ . When a  $\text{CO}_2$ -saturated methanolic solution was used the reaction was completed again instantaneously, and so the kinetics of the fast  $\text{CO}_2$  fixation reaction could not be followed. It is proposed that the conversion of the high-spin complex **1** to the reactive low-spin square planar species is initiated by the deprotonation of water molecule coordinated to Ni(II) trans to the central N2 nitrogen atom of 3N ligand upon adding  $\text{Et}_3\text{N}$  base, which is followed by the loss of two weakly coordinated water molecules oriented in directions opposite to each other (Scheme 1). As the Ni(II)-bound hydroxyl group in the reactive intermediate  $[\text{Ni}(\text{3N})(\text{OH})]^+$  is polarized and stabilized in basic medium, its electron-rich nucleophilic oxygen atom, as revealed by the HOMO of intermediates (Fig. 6), attacks the nucleophilic carbon atom of  $\text{CO}_2$  to form the carbonate bound to the mononuclear Ni(II) species  $[\text{Ni}(\text{3N})(\text{H}_2\text{O})(\text{OCO}_2)]^+$ . The monodentatively coordinated carbonate in the latter readily binds to Ni(II) in another molecule of the reactive intermediate  $[\text{Ni}(\text{3N})(\text{OH})]^+$  opposite to the sterically hindering diazepane ring, which is followed by protonation of the hydroxyl group in the latter, to form the dimeric carbonate-bound Ni(II) complex **3** as the final product. The mechanism proposed is very similar to the generally accepted carbonic anhydrase mechanism mediated by Zn(II) in the presence of a base. The deprotonation of the Zn(II)-coordinated water molecule generates a hydroxide ion bound to tetrahedral Zn(II) ( $d^{10}$ ), the



**Scheme 1** Proposed reaction pathway for fixation of atmospheric  $\text{CO}_2$  using  $[\text{Ni}(\text{L1}/\text{L2})(\text{H}_2\text{O})_2]^{2+}$  in the presence of  $\text{Et}_3\text{N}$  in methanol solution forming the reactive intermediates  $[(\text{L1}/\text{L2})\text{Ni}-\text{OH}]^+$  and  $[(3\text{N})\text{Ni}(\text{H}_2\text{O})(\text{OCO}_2)]^+$  and then carbonato-bridged dinickel(II) complex

oxygen atom of which acts as a nucleophile for the electrophilic carbon atom of  $\text{CO}_2$  in the most-efficient physiologically important enzymatic hydration of  $\text{CO}_2$  to form bicarbonate.<sup>47</sup> Similarly, the present square planar  $[(3\text{N})\text{Ni}-\text{OH}]^+$  species with Ni(II) in low-spin ( $d_{xy}, d_{xz}, d_{yz}$ )<sup>6</sup>( $d_{z^2}$ )<sup>2</sup> configuration, stabilized by the meridionally and hence strongly coordinated diazepane ligand, the Ni(II)-bound hydroxide acts as a better nucleophile for the electrophilic carbon atom of  $\text{CO}_2$  in the minimal reaction  $[(3\text{N})\text{Ni}-\text{OH}]^+ + \text{CO}_2 \rightarrow [(3\text{N})\text{Ni}(\text{H}_2\text{O})(\text{OCO}_2)]^+$ . Thus, the extremely high reactivity of the in situ generated  $[\text{Ni}(3\text{N})(\text{OH})]^+$  species is ascribed to its square planar configuration with the  $\sigma$ -electron density exposed. Similar mononuclear square planar  $[(\text{L3})\text{Ni}^{\text{II}}-\text{OH}]^-$  complexes (cf. above), have been isolated and the kinetics and mechanistic study of its fast  $\text{CO}_2$  fixation reaction in DMF has been studied in detail.<sup>22-24</sup> One might indeed expect the formation of transient bicarbonate complex  $[(3\text{N})\text{Ni}(\text{H}_2\text{O})(\text{OC}(\text{O})\text{OH})]$  via Lindskog mechanism,<sup>48</sup> which subsequently reacts with the cationic species  $[(3\text{N})\text{Ni}-\text{OH}]^+$  to form the bridging carbonate dimer. Thus, it is clear that a meridionally bound tridentate 3N ligand system suitable to confer a low-spin square planar geometry on Ni(II) in  $[(\text{L1}/\text{L2})\text{Ni}(\text{II})-\text{OH}]$  complexes is essential to enhance the nucleophilicity of the Ni(II)-bound hydroxyl group that directly takes part in  $\text{CO}_2$  activation. It has been observed<sup>21</sup> that the *t*BuDPA ligand changes from facial to meridional coordination when its Ni(II)-OH complex activates  $\text{CO}_2$  and in fact, both the modes of ligand coordination have been observed in the X-ray

crystal structure of the tetrameric 'dimer of dimer' complex  $[\text{Ni}_4(\text{tBuDPA})_4(\mu\text{-CO}_3)_2(\text{H}_2\text{O})_4](\text{ClO}_4)_4$ . It is interesting to note that the electron density in the LUMO of **2a** is distributed on the ligand orbitals as well as Ni(II)  $d_{x^2-y^2}$  orbital; however, in **1a** (Fig. 6) the LUMO is localized on pyridyl ring, and the LUMO+1 only contains electron density distributed over all the ligands as well as on the  $d_{x^2-y^2}$  orbital of Ni(II) similar to the LUMO of **2a**. The HOMO – LUMO energy gap (4.6307 eV) in **2a** is lower than the HOMO – LUMO+1 energy gap (4.7103 eV) in **1a** (Fig. 7) by 1.83 kcal mole<sup>-1</sup>, which correlates well with the higher energy needed for the conversion of low-spin **1a** to an octahedral complex **3** with high-spin Ni(II) configuration, which involves de-pairing of the two electrons in  $d_{z^2}$  orbital in **1a** and promoting one of them to the  $d_{x^2-y^2}$  orbital in **3**. This illustrates the observed lower reactivity of **1a** in fixing  $\text{CO}_2$ .

#### Catalytic conversion of $\text{CO}_2$ into Cyclic Carbonate

The ability of the  $\mu$ -carbonate complex **3** to catalyze the conversion of  $\text{CO}_2$  to cyclic carbonate was investigated in the more soluble  $\text{CH}_3\text{CN}$  as solvent at 30, 40, 50, 60 and 80 °C over a period of 8 h, by following the already reported procedure.<sup>25</sup> Styrene epoxide (5 mmol) was used as the substrate and reacted with atmospheric  $\text{CO}_2$  (1 bar) and pure  $\text{CO}_2$  at a catalyst load of 0.05 mol% and 2 equivalents of  $\text{Et}_3\text{N}$  as a base in the absence of a co-catalyst. The product was identified by using <sup>1</sup>H and <sup>13</sup>C NMR as phenylethylene carbonate (4-phenyl-1,3-dioxolan-2-one) as the major one, further confirmed by GC-MS ( $m/z$ , 164.1) and quantified by GC-MS/GC technique.

The yields were 9-15% with excellent selectivity (>99%) at the catalyst load of 0.05 mol% at ambient temperature and pressure (1 bar). The blank reaction performed only in the presence of Et<sub>3</sub>N showed the formation of only a very trace amount of the cyclic carbonate. When pure CO<sub>2</sub> (1 atm) was used the product yield increased. When the temperature was increased the yield also gradually increased: 9 (30), 25 (40), 39 (50), 55 (60), 72% (80 °C) (Table S5), without any change in the selectivity under the same experimental conditions. Thus, the reaction temperature and pressure of CO<sub>2</sub> have a strong influence on the catalytic CO<sub>2</sub> fixation reaction.

## Conclusions

Thus, the octahedral nickel(II) complexes of two diazepane-based 3N ligands [Ni(L1/L2)(H<sub>2</sub>O)<sub>3</sub>]<sup>2+</sup> generate the intermediate complex species [(L1/L2)Ni-OH]<sup>+</sup> in methanolic solution upon adding Et<sub>3</sub>N. The intermediates are highly reactive capturing CO<sub>2</sub> in the atmosphere spontaneously at ambient conditions to form the μ-carbonato dinickel(II) complex with each Ni(II) having a distorted octahedral geometry. The meridionally coordinated 3N ligands stabilize the low-spin square planar configuration of the intermediate, which is a prerequisite to render the Ni-OH moiety more nucleophilic. The complex [Ni(L2)(H<sub>2</sub>O)<sub>3</sub>]<sup>2+</sup> with electron-releasing imidazole donor produces the intermediate produced by more reactive than its pyridine analogue [Ni(L1)(H<sub>2</sub>O)<sub>3</sub>]<sup>2+</sup>. DFT studies illustrate the role of meridional coordination of the 3N ligand in causing the difference in reactivity. The μ-carbonato complex acts as an efficient catalyst in converting styrene epoxide into its cyclic carbonate using pure CO<sub>2</sub> in high yield and with excellent selectivity. More detailed kinetic and mechanistic study of the fast CO<sub>2</sub> fixation reaction and investigation of the ability of the μ-carbonato complex to involve in catalysis are under progress.

## Author Contributions

Almost all the work is carried out by Mr. T. Ajaykamal and Prof. M. Palaniandavar at School of Chemistry, Bharathidasan University, Tiruchirappalli 620024, Tamil Nadu, India. Professor Islam and Mitu Sharma collected the X-ray structure data at Tezpur University, Tezpur, Assam, India for complex **3**.

## Conflicts of interest

There are no conflicts to declare.

## Acknowledgements

We thank Indian National Science Academy (INSA), New Delhi, for the INSA Senior Scientist position to M.P. and the Science and Engineering Research Board (SERB), New Delhi for a research project with financial support (EMR/2015/002222) to M. P. HR-MS facility sanctioned to School of Chemistry, Bharathidasan University through DST-FIST is acknowledged.

Mr. Aditya Borah, Department of Chemistry, IITB, Mumbai is thanked for help in solving the X-ray structure. We thank Dr. M. Murali, National College, Tiruchirappalli, for the electrochemical measurement facility.

## Notes and references

- (a) S. M. Glueck, S. Gumus, W. M. F. Fabian, K. Faber, *Chem. Soc. Rev.*, 2010, **39**, 313. (b) T. Sakakura, J. C. Choi, H. Yasuda, *Chem. Rev.*, 2007, **107**, 2365. (c) D. J. Darensbourg, *Inorg. Chem.*, 2010, **49**, 10765. (d) X. Li, J. Yu, M. Jaroniec, X. Chen, *Chem. Rev.*, 2019, **119**, 3962–4179.
- (a) P. A. Lindahl, *Biochemistry*, 2002, **41**, 2097. (b) P. Woolley, *Nature*, 1975, **258**, 677.
- E. Kimura, *Acc. Chem. Res.*, 2001, **34**, 171.
- (a) M. Aresta, A. Dibenedetto, A. Angelini, *Chem. Rev.*, 2014, **114**, 1709. (b) D. A. Palmer, R. V. Eldik, *Chem. Rev.*, 1983, **83**, 651. (c) S. Krogsrud, S. Komiya, T. Ito, J. A. Ibers, A. Yamamoto, *Inorg. Chem.*, 1976, **15**, 2798. (d) D. H. Gibson, *Chem. Rev.*, 1996, **96**, 2063.
- S. Diekmann, J. Weston, E. Anders, W. Boland, B. Schonecker, T. Hettmann, J. von Langen, S. Erhardt, M. Mauksch, M. Brauer, C. Beckmann, M. Rost, P. Sperling, E. Heinz, *Nature Rev. Mol. Biotechnol.*, 2002, **90**, 73.
- N. J. English, M. M. El-Hendawy, D. A. Mooney, J. M. D. MacElroy, *Coord. Chem. Rev.*, 2014, **269**, 85.
- M. Mikkelsen, M. Jorgensen, F. C. Krebs, *Energy Environ. Sci.*, 2010, **3**, 43.
- K. M. Merz, R. Hoffmann, M. J. S. Dewar, *J. Am. Chem. Soc.*, 1989, **111**, 5636.
- V. M. Krishnamurthy, G. K. Kaufman, A. R. Urbach, I. Gitlin, K. L. Gudiksen, D. B. Weibel, G. M. Whitesides, *Chem. Rev.*, 2008, **108**, 946.
- J. H. Jeoung, H. Dobbek, *Science*, 2007, **318**, 1461.
- A. Parkin, J. Seravalli, K. A. Vincent, S. W. Ragsdale, F. A. Armstrong, *J. Am. Chem. Soc.*, 2007, **129**, 10328.
- P. A. Karplus, M. A. Pearson and R. P. Hausinger, *Acc. Chem. Res.*, 1997, **30**, 330–337.
- (a) F. D. Monica, S. V. C. Vummaleti, A. Buonerba, A. De Nisi, M. Monari, S. Milione, A. Grassi, L. Cavallo, C. Capacchione, *Adv. Synth. Catal.*, 2016, **358**, 3231. (b) A. Buchard, M. R. Kember, K. G. Sandeman, C. K. Williams, *Chem. Commun.*, 2011, **47**, 212. (c) D. Alhashmialameer, J. Collins, K. Hattenhauer, F. M. Kerton, *Catal. Sci. Technol.*, 2016, **6**, 5364.
- (a) M. A. Fuchs, T. A. Zevaco, E. Ember, O. Walter, I. Held, E. Dinjus, M. Döring, *Dalton Trans.*, 2013, **42**, 5322. (b) C. J. Whiteoak, E. Martin, M. M. Belmonte, J. Benet-Buchholz, A. W. Kleij, *Adv. Synth. Catal.*, 2012, **354**, 469. (c) E. Fazekas, G. S. Nichol, M. P. Shaver, J. A. Garden, *Dalton Trans.*, 2018, **47**, 13106. (d) C. K. Karan, M. Bhattacharjee, *Inorg. Chem.*, 2018, **57**, 4649.
- H. Dobbek, L. Gremer, R. Kiefersauer, R. Huber, O. Meyer, *Proc. Natl. Acad. Sci. U. S. A.*, 2002, **99**, 15971.
- (a) C. K. Karan, M. C. Sau, M. Bhattacharjee, *Chem. Commun.*, 2017, **53**, 1526. (b) P.-Z. Li, X.-J. Wang, J. Liu, J. S. Lim, R. Zou, Y. Zhao, *J. Am. Chem. Soc.*, 2016, **138**, 2142.
- F. Möller, K. Merz, C. Herrmann and U. P. Apfel, *Dalton Trans.*, 2016, **45**, 904–907
- E. Carmona, J. M. Marin, P. Palma, M. Paneque, and M. L. Poveda, *Inorg. Chem.*, 1989, **28**, 1895-1900.
- N. Kitajima, S. Hikichi, M. Tanaka and Y. Moro-oka, *J. Am. Chem. Soc.*, 1993, **115**, 5496-5508.
- M. Ito, Y. Takita, *Chem. Lett.*, 1996, 929-930.
- J. P. Wikstrom, A. S. Filatov, E. A. Mikhalyova, M. Shatruk, B. M. Foxman and E. V. R. Akimova, *Dalton Trans.*, 2010, **39**, 2504–2514.

- 22 D. Huang, O. V. Makhlynets, L. L. Tan, S. C. Lee, E. V. R. Akimova, and R. H. Holm, *Proc. Natl. Acad. Sci. U. S. A.*, 2011, **108**, 1222–1227.
- 23 D. Huang, O. V. Makhlynets, L. L. Tan, S. C. Lee, E. V. R. Akimova, and R. H. Holm, *Inorg. Chem.*, 2011, **50**, 10070–10081.
- 24 O. Troeppner, D. Huang, R. H. Holm and I. I. Burmazović, *Dalton Trans.*, 2014, **43**, 5274–5279.
- 25 S. Muthuramalingam, M. Sankaralingam, M. Velusamy, and R. Mayilmurugan, *Inorg. Chem.*, 2019, **58**, 12975–12985.
- 26 M. Mondal, J. Mayans, A. Ghosh, *Inorg. Chim. Acta.*, 2019, **498**, 119175.
- 27 (a) W. Guo, J. E. Gómez, À. Cristòfol, J. Xie, A. W. Kleij, *Angew. Chem., Int. Ed.*, 2018, **57**, 13735. (b) F. D. Bobbink, F. Menoud, P. J. Dyson, *ACS Sustainable Chem. Eng.*, 2018, **6**, 12119. (c) J. H. Clements, *Ind. Eng. Chem. Res.*, 2003, **42**, 663.
- 28 (a) J. A. Castro-Osma, J. W. Comerford, S. Heath, O. Jones, M. Morcillo, M. North, *RSC Adv.*, 2015, **5**, 3678. (b) M. Morcillo, M. North, P. Villuendas, *Synthesis*, 2011, **12**, 1918. (c) H. L. Parker, J. Sherwood, A. J. Hunt, J. H. Clark, *ACS Sustainable Chem. Eng.*, 2014, **2**, 1739. (d) I. Omae, *Catal. Today.*, 2006, **115**, 33.
- 29 S. Phadke, M. Cao, M. Anouti, *ChemSusChem.*, 2018, **11**, 965.
- 30 T. Dhanalakshmi, E. Suresh, H. S. Evans and M. Palaniandavar, *Eur. J. Inorg. Chem.*, 2006, 4687–4695.
- 31 R. Mayilmurugan, H. S. Evans and M. Palaniandavar, *Inorg. Chem.*, 2008, **47**, 6645.
- 32 T. Dhanalakshmi, E. Suresh and M. Palaniandavar, *Inorg. Chim. Acta.*, 2011, **365**, 143–151.
- 33 M. Velusamy, R. Mayilmurugan, M. Palaniandavar, *J. Inorg. Biochem.*, 2005, **99**, 1032–1042.
- 34 M. Velusamy, M. Palaniandavar and K. R. J. Thomas, *Acta Cryst.*, 1998, **17**, 2179–2186.
- 35 M. Palaniandavar, R. J. Butcher and A. W. Addison, *Inorg. Chem.*, 1996, **35**, 467–471.
- 36 B. Horn, C. Limberg, C. Herwig and B. Braun, *Chem. Comm.*, 2013, **49**, 10923–10925.
- 37 M. Sankaralingam, M. Balamurugan, M. Palaniandavar, *Coord. Chem. Rev.*, 2020, **403**, 213085.
- 38 M. Sankaralingam, P. Vadivelu and M. Palaniandavar, *Dalton Trans.*, 2017, **46**, 7181–7193.
- 39 (a) R. Loganathan, S. Ramakrishnan, E. Suresh, A. Riyasdeen, M. A. Akbarsha, and M. Palaniandavar, *Inorg. Chem.*, 2012, **51**, 5512–5532. (b) R. Loganathan, M. Ganeshpandian, N. S. P. Bhuvanesh, M. Palaniandavar, A. Muruganatham, S. K. Ghosh, A. Riyasdeen, M. A. Akbarsha, *J. Inorg. Biochem.*, 2017, **174**, 1–13.
- 40 M. Velusamy, M. Palaniandavar and K. R. J. Thomas, *Polyhedron*, 1998, **17**, 2179.
- 41 G. M. Sheldrick, *Acta Cryst.*, 2015, **71**, 3–8.
- 42 M. N. Burnett, C. K. Johnson, ORTEP III, Oak Ridge Thermal Ellipsoid Plot Program for Crystal Structure Illustrations, Report ORNL-6895, Oak Ridge National Laboratory, Oak Ridge, TN, 1996.
- 43 M. J. Frisch, G. W. Trucks, H. B. Schlegel, G. E. Scuseria, M. A. Robb, J. R. Cheeseman, G. Scalmani, V. Barone, B. Mennucci, G. A. Petersson, H. Nakatsuji, M. Caricato, X. Li, H. P. Ratchian, A. F. Izmaylov, J. Bloino, G. Zheng, J. L. Sonnenberg, M. Hada, M. Ehara, K. Toyota, R. Fukuda, J. Hasegawa, M. Ishida, T. Nakajima, Y. Honda, O. Kitao, H. Nakai, T. Vreven, J. A. Montgomery, Jr., J. E. Peralta, F. Ogliaro, M. Bearpark, J. J. Heyd, E. Brothers, K. N. Kudin, V. N. Staroverov, R. Kobayashi, J. Normand, K. Raghavachari, A. Rendell, J. C. Burant, S. S. Iyengar, J. Tomasi, M. Cossi, N. Rega, J. M. Millam, M. Klene, J. E. Knox, J. B. Cross, V. Bakken, C. Adamo, J. Jaramillo, R. Gomperts, R. E. Stratmann, O. Yazyev, A. J. Austin, R. Cammi, C. Pomelli, J. W. Ochterski, R. L. Martin, K. Morokuma, V. G. Zakrzewski, G. A. Voth, P. Salvador, J. J. Dannenberg, S. Dapprich, A. D. Daniels, O. Farkas, J. B. Foresman, J. V. Ortiz, J. Cioslowski, D. J. Fox, Gaussian 09, Revision A.1, Gaussian, Inc., Wallingford CT, 2009.
- 44 A. D. Becke, *J. Chem. Phys.*, 1993, **98**, 1372.
- 45 P. J. Hay, W. R. Wadt, *J. Chem. Phys.*, 1985, **82**, 270–283.
- 46 P. J. Hay, W. R. Wadt, *J. Chem. Phys.*, 1985, **82**, 299–310.
- 47 (a) A. Looney, G. Parkin, R. Alsfasser, M. Ruf, and H. Vahrenkamp, *Angew. Chem. Int. Ed. Engl.*, 1992, **31**, 92–93. (b) M. Ruf, F. A. Schell, R. Walz, and H. Vahrenkamp, *Chem. Ber.*, 1997, **130**, 101–104. (c) H. Vahrenkamp, *Dalton Trans.*, 2007, 4751–4759.
- 48 S. Lindskog and J. E. Coleman, *Proc. Natl. Acad. Sci. U. S. A.*, 1973, **70**, 2505–2508.
- 49 D. F. Evans, D. A. Jakubovic, *J. Chem. Soc. Dalton Trans.* 1988, 2927–2933.